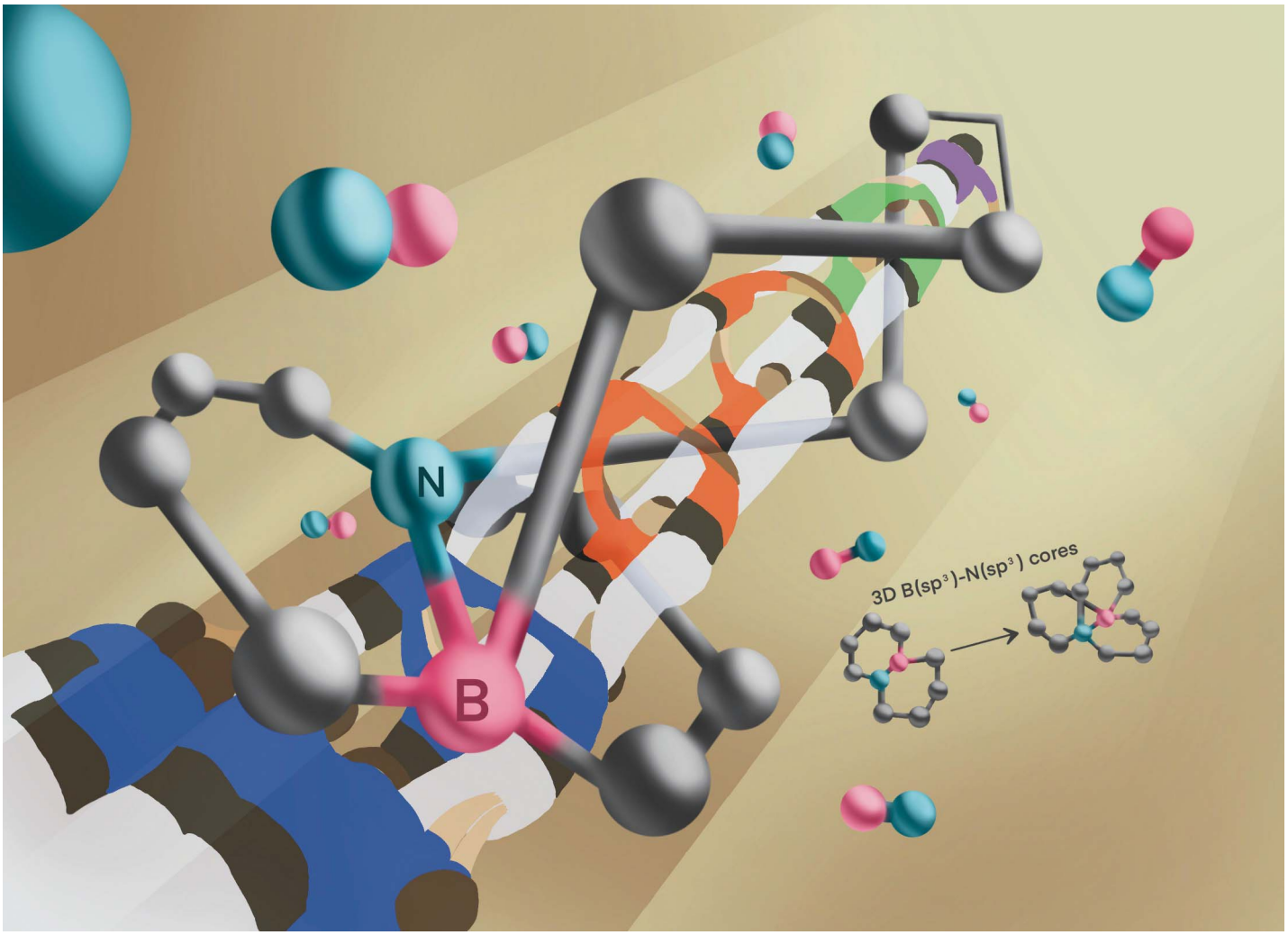

Showcasing research from the BISi-Bonds/CRISOL laboratory of Dr. Shafir and Dr. Cuenca, IQAC-CSIC and IQS-URL, Barcelona, Spain.

B–N axis as a facilitating agent for the synthesis of 3D structures: the paradigmatic case of BN-[4.4.4]propellane

While BN-isosterism has come under spotlight as a tool for diversifying and tuning 2D π-extended organic structures, systematic BN-mapping of 3D sp^3–sp^3 architectures remains largely unexplored. This work presents a direct pathway to such 3D BN-cores by disrupting the π-bond of a B═N unit. A BN-centered [4.4.4]propellane is rapidly assembled through polar B═N 1,2-diallylation, followed by a stereoconvergent ring-closing metathesis to forge the propellane cage. The cover art, inspired by the intricate framework of traditional Catalan *castellers* human towers, reflects this cooperative three-ring construction.

Image reproduced by permission of Alexandr Shafir from *Chem. Sci.*, 2025, **16**, 22970. Image created by Carla Diaz @carladisal.

As featured in:

See Ana B. Cuenca, Alexandr Shafir *et al.*, *Chem. Sci.*, 2025, **16**, 22970.

ROYAL SOCIETY OF CHEMISTRY

15 YEARS ANNIVERSARY

rsc.li/chemical-science

Registered charity number: 207890

Chemical Science

ROYAL SOCIETY OF CHEMISTRY

EDGE ARTICLE

View Article Online
View Journal | View Issue

Cite this: *Chem. Sci.*, 2025, **16**, 22970

All publication charges for this article have been paid for by the Royal Society of Chemistry

B–N axis as a facilitating agent for the synthesis of 3D structures: the paradigmatic case of BN-[4.4.4] propellane

Guillem Sanz-Liarte, [ac] Josep Saurí, [b] Pau Nolis, [d] Ana B. Cuenca *[be] and Alexandr Shafir *[ae]

Received 10th July 2025
Accepted 21st October 2025

DOI: 10.1039/d5sc05132k

rsc.li/chemical-science

Flat aromatic compounds containing a boron–nitrogen (BN) fragment have gained significant attention in the field of organic optoelectronics. Unsurprisingly, therefore, an increasing number of synthetic methodology groups have devoted efforts and creativity to developing new strategies for accessing diverse structures incorporating a B=N unit, which is isosteric with the olefinic C=C bond. In contrast, the potential of BN isosterism to expand the structural diversity of three-dimensional architectures based on sp^3-hybridized atoms remains largely underexplored. In this study, we introduce a strategy to construct an alkane-type quaternary–quaternary Bsp^3–Nsp^3 molecular axis *via* double addition of a carbon-based nucleophile/electrophile pair to a readily accessible olefin-type B=N moiety. The approach is showcased through the synthesis of a BN-[4.4.4]-propellane, in which the rapidly assembled tetrahydro-BN-naphthalene intermediate undergoes a polar double allylation of its B=N bond. Despite the unfavorable *trans* preference in this addition step, efficient [4.4.4]-propellane formation was achieved through a tandem metathesis-based *trans*-to-*cis* isomerization and ring-closing reaction. The resulting BN-propellane exhibits a C_3-symmetric helical arrangement in the solid state and shows fluxional behavior in the ^1H NMR spectrum at room temperature due to a helicity flip, for which variable-temperature NMR measurements yielded an activation barrier ($\Delta G^{\ddagger}$) of approximately 14.6 kcal mol^{-1}.

BN-isosterism involves replacing a carbon–carbon (C–C) bond with a boron–nitrogen (B–N) fragment, taking advantage of the fact that both pairs possess eight valence electrons, which allows for analogous Lewis structures and similar molecular geometries. At the same time, the substitution transforms the low-polarity CC unit into a strongly polarized BN bond, thereby altering the compound's orbital energies, reactivity and physical properties (Scheme 1A).[1,2] Owing to its potential for electronic tuning of polycyclic aromatic compounds,[3] 1,2-BN isosterism is viewed as a transformative tool in the field of organic optoelectronics,[4,5] prompting significant synthetic efforts toward flat structures containing olefin-type B=N units isosteric with a C=C fragment.[6] In contrast, very little systematic research exists on the preparation and properties of non-trivial 3D molecules incorporating sp^3–sp^3 BN moieties mimicking saturated alkane C–C bonds.

This disparity between the attention received by sp^2-*vs.*-sp^3 type BN compounds stands in sharp contrast to the growing synthetic emphasis – outside of BN isosterism – on highly

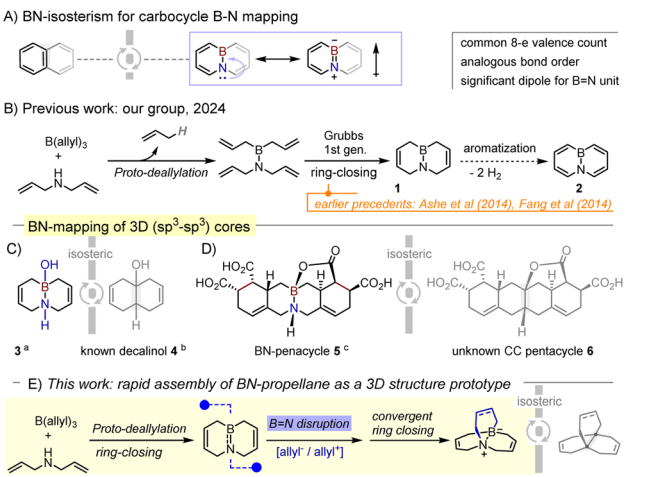

Scheme 1 Precedents in the formation of the B=N bicycle **1**, and the relevant isosteric analogy between B–N and C–C sp^3–sp^3 cores. [a]Ref. 8b; our unpublished work; [b]ref. 10; [c]ref. 9.

[a]*BISi-Bonds group, Department of Biological Chemistry, Institut de Química Avançada de Catalunya, IQAC-CSIC, c/Jordi Girona 20, 08034 Barcelona, Spain. E-mail: alexandr.shafir@iqac.csic.es*

[b]*BISi-Bonds/CRISOL group, Department of Organic and Pharmaceutical Chemistry, Institut Químic de Sarrià, Universitat Ramon Llull, Vía Augusta 390, 08017 Barcelona, Spain. E-mail: anabelen.cuenca@iqs.url.edu*

[c]*Departament de Química Inorgànica i Orgànica, Universitat de Barcelona, 08028, Barcelona, Spain*

[d]*Servei de Ressonància Magnètica Nuclear, Universitat Autònoma de Barcelona, Bellaterra, 08193, Barcelona, Spain*

[e]*Centro de Innovación en Química Avanzada (ORFEO-CINQA), Barcelona, Spain*

substituted sp^3-hybridized carbon atoms underpinning three-dimensional molecular architectures. Much of the latter interest is fuelled by the escape-from-the-flatland campaign, where a shift away from planar aromatic scaffolds and toward sp^3-rich, 3D structures is seen as venturing to the under-populated corners of chemical space and enhancing drug discovery.[7] In this regard, it would be compelling to readily map diverse carbon-based 3D architectures onto their BN isosteres, anywhere from simpler linear and cyclic molecular cores, to more elaborate spirocycles, cages or propellanes. An interesting possibility that got our attention is to generate saturated 3D structures *via* di-functionalization of the more synthetically available (*vide supra*) olefin-like type B=N axes. This idea was inspired by earlier work on the bicyclic aminoborane **1** (Scheme 1B), first prepared by the Ashe and Fang groups on route to BN-naphthalene **2**,[8] and recently revisited by our group through a robust multigram synthesis featuring quantitative condensation of $B(allyl)_3$ with *N*,*N*-diallylamine, followed by ring-closing olefin metathesis (Scheme 1B).[9] Importantly, while **1** is generally handled under an inert atmosphere, reflecting the general challenge of working with non-aromatic (and, often, even aromatic) B=N derivatives, its B–N hydrate **3**[8b] proved to be air- and moisture-stable, foreshadowing greater stability of the sp^3–sp^3 BN derivatives. In terms of isosterism, while **1** maps onto 1,4,5,8-tetrahydronaphthalene, its hydrate **3** is isosteric with the known decalinol **4** (Scheme 1C).[10] Our studies also reveal the potential for generating higher structural complexity, as illustrated by the air- and moisture-stable BN-pentacycle **5**, formed *via* intramolecular addition of a carboxylic acid across a B=N bond in a Diels–Alder-derived tetracyclic B=N precursor; the product is a BN isostere of the hitherto unreported pentacycle **6** (Scheme 1D).[9] In the present study, the concise synthesis of air- and moisture-stable BN-[4.4.4]-propellane is used to show that B=N double functionalization represents a broader strategy for BN-mapping of 3D structure (Scheme 1E).

Indeed, while compounds **3** and **5** shown in Scheme 1 represent a reaction between B=N and a $[H^+/OR^-]$ pair, we envisaged that analogous chemistry can potentially also extend to C-based nucleophile/electrophile combinations. Given the lower π-contribution[11] and higher polarization in the B=N moiety, disrupting its π component should be considerably easier than in the non-activated C=C moiety. Thus, in light of the appeal of the propellane structure motif, both as a synthetic challenge and as a component of functional materials,[12] this report explores and validates the B=N π-disruption strategy through rapid elaboration of the air- and moisture-stable BN-[4.4.4]-propellane. The process entails a polar (Nu^-/E^+) di-allylation of the B=N group followed by endgame ring-closing metathesis of intermediate **7** (Scheme 2).

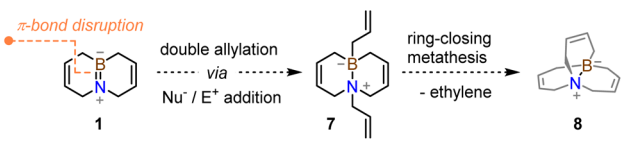

Scheme 2 The proposed double B=N allylation as a strategy towards a propellane core.

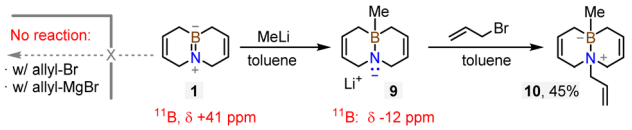

Scheme 3 Initial exploration of disrupting the B=N π-donation for double functionalization.

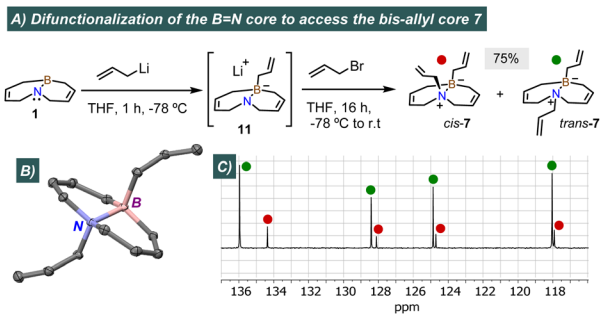

Scheme 4 Formation and characterization of the bis-allyl structure **7**. (A) The double B=N allylation of **1** through B=N π-disruption with allyl-lithium. (B) X-ray crystal structure (ORTEP-type) of *trans*-**7** at 50% thermal ellipsoids; H atoms omitted; (C) ^{13}C NMR of **7**.

Multigram quantities of bicycle **1** required in this study were readily procured *via* one-pot solvent-free condensation of $B(allyl)_3$ with the *N*,*N*-diallylamine, followed by ring closing metathesis, as described earlier by our laboratory (see Scheme 1 and SI).[9]

Initial attempts to engage **1** either through *N*-alkylation with allyl bromide, or through *B*-quaternization with allyl magnesium reagents, were unsuccessful (Scheme 3, left), reflecting a still considerable *N*-to-*B* π-donation. Nevertheless, taking note of recent precedents from the Szymczak group[13] and the laboratory of García-García and Vaquero[14] on the B-quaternization of related BN-bicycles, we proceeded to test the more nucleophilic organolithium reagents. Indeed, control experiments with MeLi did produce a quaternized B center, as evidenced by the ^{11}B NMR resonance shifting from 41 ppm to −12 ppm (Scheme 3, right). The resulting B–Me anion **9** now readily underwent *N*-alkylation with allylbromide to give the B_{sp^3}–N_{sp^3} aminoborane **10** in 45% yield as a white solid.

Applying this approach to the target *B*,*N*-diallylation, a treatment of **1** with freshly prepared allyllithium[15] at −78 °C in THF afforded the *B*-allyl anion **11**, which was quenched with allyl bromide to give the di-allyl target **7** (Scheme 4A). Compound **7** could now be handled without special precautions, and was isolated as a white crystalline solid in 75% yield by conventional column chromatography on silica gel using hexane as eluent. The structure was supported by ^1H, ^{13}C and ^{11}B NMR, the lattermost giving a sharp peak at −3.30 ppm for the quaternized boron center.

The NMR of **7** showed a mixture of two stereoisomers in an 85/15 ratio, with the X-ray crystal structure of the major component revealing a *trans*-BN-decalin disposition (Scheme 4B and C). With only the minor *cis* isomer correctly disposed for

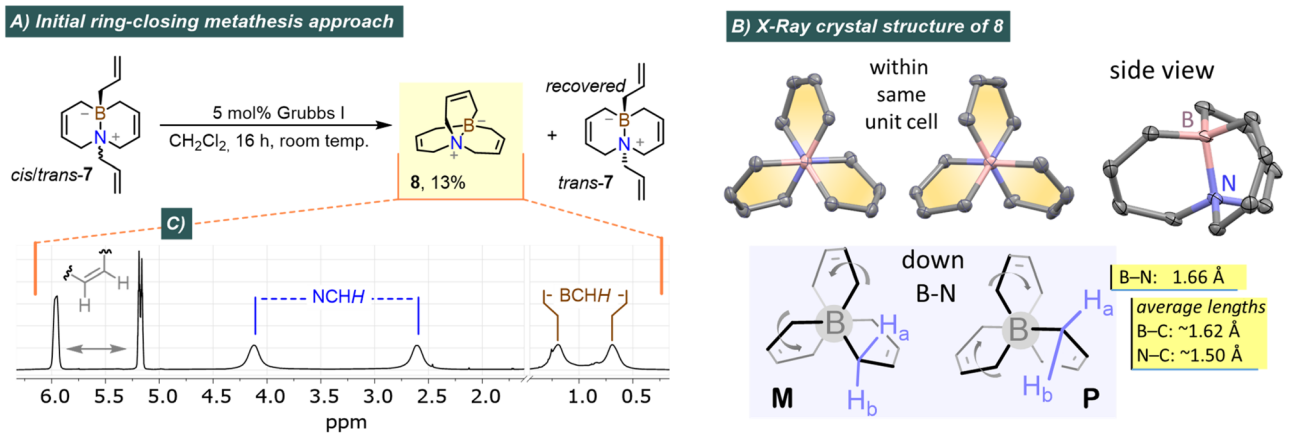

Scheme 5 (A) Initial test to form propellane **8**, (B) ORTEP diagram of the X-ray structure of **8** at 50% thermal ellipsoids. (C) ^{1}H NMR of **8**.

ring closing, this stereochemical outcome posed a challenge to our endgame strategy. To test if at least the minor *cis* fraction is effective under ROM conditions, **7** – used as an isomer mixture – was subjected to the 1st generation Grubbs catalyst (**G-I**, 5 mol%) in CH_2Cl_2. After 16 h at room temperature, the *cis* isomer was selectively consumed, leading to the formation of the target BN-[4.4.4]propellane **8**, while the *trans*-**7** remained unreacted (Scheme 5A). Compound **8** was identified by its GC-MS molecular ion at $m/z = 187$, and was isolated as a stable, colorless crystalline solid in 13% yield—consistent with the 15% initial abundance of the reactive *cis* isomer in the mixture. The C_3 symmetry of **8** is reflected in its four-resonance ^{13}C NMR spectrum, where the two olefinic peaks at 133 and 118 ppm are complemented by the two aliphatic resonances at 56 (NCH_2) and 21 ppm (BCH_2).

Crystals of **8** suitable for X-ray diffraction were grown by slow evaporation of a hexane solution. The X-ray crystal structure of **8** (Scheme 5B) confirms the expected molecular C_3-symmetry with a helical propeller-like arrangement of the three 6-membered lobes around the saturated B–N axis. While each individual molecule is thus chiral due to its propeller twist, the non-chiral (centrosymmetric) space group of $P2_a/c$ leads to the unit cell containing both enantiomers. Applying the helix chirality descriptors *M* and *P*, we can see that the left structure in Scheme 5B possesses a left-handed screw arrangement, thus giving it an *M* configuration, while the structure on the right is *P* due to its right-handed screw arrangement. The twist is duly reflected by the ^{1}H NMR of **8**, as shown in Scheme 5C, where the chair-like geometry of each 6-membered blade leads to distinguishable axial and equatorial CH positions in the CH_2 groups. The spectrum features two CH_2 groups, each as a diastereotopic pair of broad singlets: at 4.12 and 2.61 ppm for NCH_2, and at 1.19 and 0.69 ppm for BCH_2. Considering the helicity of the propellane core, this fluxional behaviour, as evidenced by such peak broadening, signals an interconversion (*via* a ring flip) of the two enantiomeric forms on the NMR timescale, leading to an exchange between axial and equatorial C–H positions, also illustrated in the lower part of Scheme 5B. For the 3D structure, a comparison with the crystal structure of the carbocyclic analogue **SI-1** (see the SI), synthesized by Altman and co-workers in 1967 and analyzed by the Dunitz laboratory in 1971,[16,17] revealed subtle structural differences between the two isosteres, most notably in the elongation of the central axis from 1.55 Å for C–C to 1.66 Å for the B–N.

Seeking to overcome the unfavorable stereochemistry produced in the B–N diallylation of **1**, we explored the possibility of implementing a metathesis-based *cis–trans* isomerization of **7**. We envisioned that a sufficiently potent metathesis catalyst could both perform the ring closing in *cis*-**7**, and also catalyse an intramolecular metathesis between an allyl group and a ring olefin moiety in *trans*-**7** yielding the C_s-symmetric intermediate **12** (Scheme 6),[18] which could then undergo a second metathesis step to form the *cis*-**7**. The *cis–trans* equilibrium could then be driven by the ring closing of the *cis* component to propellane **8**.

As discussed above (see Scheme 5), the catalyst **G-I** proved to be ineffective for such isomerization, only showing activity for ring closing of *cis*-**7**. Nevertheless, in a further exploration with isolated *trans*-**7**, we became cautiously optimistic upon detecting trace amounts of **8** when applying the Grubbs-II catalyst (**G-II**), with even higher conversions (2–7%) observed using the 2nd generation Hoveyda–Grubbs (**HG-II**) or the 3rd generation Grubbs catalysts (**G-III**, Scheme 6, bottom).[19,20] Returning to the original *trans*/*cis*-**7** (85/15) mixture, the best-performing **HG-II**

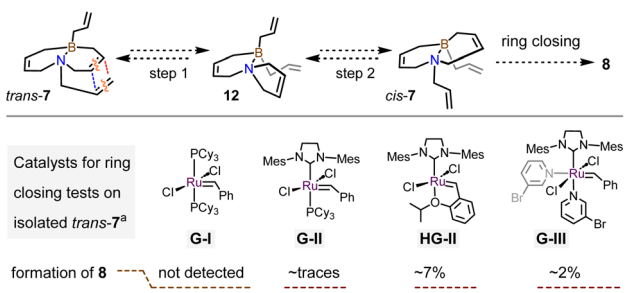

Scheme 6 Top: Mechanistic proposal for the *trans*-to-*cis* isomerization in **7**; Bottom: initial test for the isomerization-ring closing hypothesis. [a]Using 5 mol% catalyst in CH_2Cl_2 at room temperature.

Table 1 Optimization of the ring closing on *trans*/*cis*-**7**

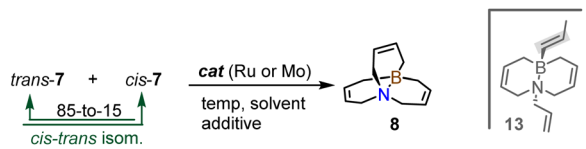

Run	Cat.	% Cat.	Solvent	T [°C]	Addit.[a]	Yield
1	**HG-II**	5 mol%	CH_2Cl_2	RT	—	20%
2	**HG-II**	10 mol%	CH_2Cl_2	RT	—	20%
3	**HG-II**	15 mol%	CH_2Cl_2	RT	*p*-BQ	15%
4	**HG-II**	15 mol%	Toluene	80	*p*-BQ	40%
5	**HG-II**	15 mol%	Toluene	110	*p*-BQ	46%
6	**HG-II**	2 × 5 mol%	Toluene	110	*p*-BQ	65%
7	**G-III**	2 × 5 mol%	Toluene	110	*p*-BQ	80%
8	**Mo-I**[b]	15 mol%	Toluene	110	—	90%

[a] Using 20 mol% of *para*-benzoquinone when indicated. [b] The **Mo-I** catalyst used in entry 8 refers to 2,6-diisopropylphenylimidoneophylidene molybdenum(VI) bis(hexafluoro-*t*-butoxide), CAS 139220-25-0.

(CH_2Cl_2, room temp., 5–10% catalyst loading) afforded a ~20% yield of **8**, *i.e.* just ~5% above the precursor's *cis* content (Table 1, runs 1 and 2). The resulting product mixture also contained species **13** arising *via* olefin double bond migration, a phenomenon associated with catalysis by Ru–H species or Ru(0) nanoparticles stemming from the degradation of the Ru carbene catalyst.[21,22] Following literature precedents, the side reaction could be suppressed through the addition of *p*-benzoquinone,[21] albeit initially without an increase in the yield of **8** (run 3).

Nevertheless, up to 40–50% yields were achieved in toluene at elevated temperatures (runs 4 and 5), reaching a 65% yield through catalyst addition in two 5% batches at 110 °C (run 6). To our delight, under the latter conditions the **G-III** catalyst, originally somewhat less active than **HG-II**, now led to the BN-[4.4.4]propellane **8** in 80% yield (run 7). A parallel study on other catalyst types also revealed an excellent performance from the Schrock Mo-based catalyst **Mo-I**,[23] which led to **8** in 90% yield, albeit with the need for rigorous air-free conditions (Table 1, run 8). The BN-[4.4.4]propellane **8** can thus be obtained from the predominantly *trans B*,*N*-diallyl precursor **7**, either employing the bench-stable **HG-II** or **G-III** catalysts, or with the air-sensitive but highly efficient Schrock-type Mo catalyst. Further stability tests for **8**, suggested by a referee, revealed that in addition to being air-and moisture stable, solutions of this propellane remain unchanged, as gauged by ^{1}H and ^{11}B NMR, after heating to 70 °C for 16 h, or after irradiation at 350 nm or 460 nm for 5 h (see the SI).

The tri-olefin **8** could be converted to saturated [4.4.4]BN-propellane **14** in 75% yield by smooth hydrogenation using Pd/C (Scheme 7, top), where this compound formed along with a minor unexpected isomer identified (see the SI) as [4.4.3]-BN-propellane **15**, ostensibly due to Pd/C-catalyzed isomerization. As was previously observed for **8**, compound **14** exhibits a fluxional ^{1}H NMR spectrum, with the molecule's helical twist (confirmed through DFT, see Scheme 7 and the SI) resulting in eight broad resonances between +4 and −1 ppm for the four chemically distinct CH_2 groups (see the SI). Preliminary exploration also reveals that the olefinic double bonds in **8** can undergo reactions such as cyclopropanation or epoxidation, albeit leading to a mixture of mono-, bis- and tris-functionalized species. For the sake of illustration, the epoxidation reaction, which can be driven to the double epoxide **16** with moderate selectivity, is shown in Scheme 7, bottom. The product is obtained in three isomer forms, as reflected by three peaks in the GC-MS, with isomers designated using "up" and "down" descriptors to indicate the direction of the epoxide units.

As previously noted, the interconversion between the enantiomeric helical forms of propellanes **8** and **14** results in a positional exchange between the equatorial and axial C–H sites in each CH_2 group. For **8**, this process was assessed by variable temperature ^{1}H NMR in toluene-d_8. While the compound's two unique CH_2 groups appeared as four broad resonances at room temperature, cooling to 228 K led to signal sharpening, with each of the four signals displaying well-resolved geminal ^2J(HH) coupling constants (16 Hz for the methylene protons α to nitrogen and 18.5 Hz for the methylene protons α to boron). As the temperature was gradually raised to 350 K, the accelerated interconversion led to the coalescence of

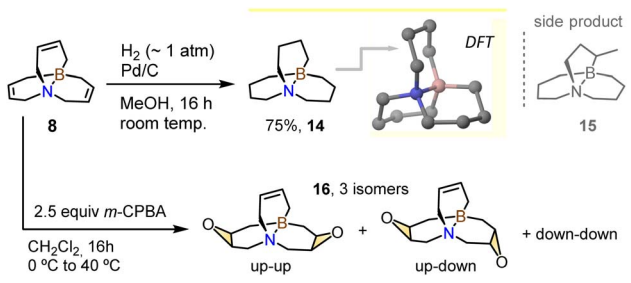

Scheme 7 Top: Transformation of **8** to the saturated BN-propellane **14**, along with its DFT-based molecular geometry (B3LYP/6-31+g(d,p)); Bottom: double epoxidation of **8** and the illustration of the three isomeric epoxide products.

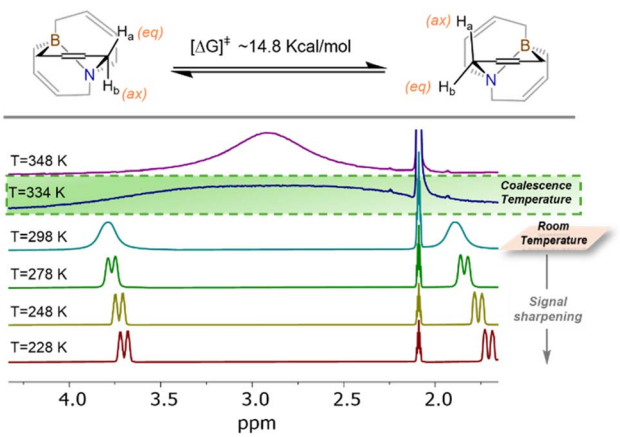

Fig. 1 Exchange process and coalescence of the N-HH resonances.

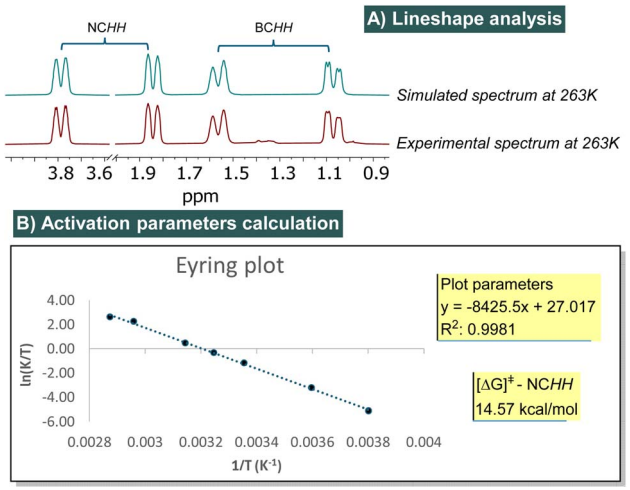

Fig. 2 (A) Simulated ^{1}H NMR spectrum obtained from DNMR at T = 263 K with a best overlap fitting obtained at 92.26%. *vs.* the experimental ^{1}H NMR spectrum at T = 263 K. (B) Eyring plot obtained for NCHH from DNMR extracted k_{ex} values.

diastereotopic pairs, initially for the more closely positioned B-CHH resonances (316 K, see the SI), and then for the wider-spaced N-CHH peaks (334 K, see Fig. 1). These coalescence temperatures (T_c) were used with the Eyring equation to calculate $\Delta G^{\ddagger}$ for the helical flip in **8**, yielding internally highly consistent values of 14.64 and 14.73 kcal mol^{-1} (see the SI).

For an even more accurate analysis, the experimental $\Delta G^{\ddagger}$ values were probed through a lineshape analysis using the DNMR software package in TopSpin (v. 4) to fit experimental *vs.* simulated spectra for each of the variable-temperature ^{1}H-NMR datapoints recorded. This procedure yielded an interconversion rate constant (k) for the methylene groups at each studied temperature (Fig. 2A). Based on these constants, Eyring plots were constructed by representing $\ln(k/T)$ against $1/T$. The resulting plots showed a strong linear correlation, described by the equation $f(x) = a + bx$, where the slope and the intercept represent $\Delta H^{\ddagger}$ and $\Delta S^{\ddagger}$, respectively. Using these data and the expression $\Delta G^{\ddagger} = \Delta H^{\ddagger} - T\Delta S^{\ddagger}$ thus allowed for the $\Delta G^{\ddagger}$ values for NHH and BHH to be calculated.

For example, as shown in Fig. 2B, the Eyring plot corresponding to the α protons to N yielded a linear regression with an R^2 value of 99.9981, from which a $\Delta G^{\ddagger}$ value of 14.57 kcal mol^{-1} was calculated. Following an analogous procedure, a $\Delta G^{\ddagger}$ value of 14.89 kcal mol^{-1} was determined for the BHH protons (see the SI). We were pleased to observe that these values closely align with those obtained experimentally, further validating our results. We note that analogous dynamic behavior had been documented by Altman *et al.* for the carbonaceous propellane **SI-1**, with the $\Delta G^{\ddagger}$ for this "helical flip" in the BN-propellane **8** being approximately 2 kcal mol^{-1} higher than that of its all-carbon isostere.[24] In contrast, this experimental barrier is almost 3 times higher than the 5–6 kcal mol^{-1} ring inversion barrier in cyclohexene, a ring representing individual lobes in propellane **8**. This is likely the result of the coordination required to flip all three rings within the same movement.[25]

In summary, this work explores the synthetic potential of the B=N sp^2–sp^2 unit as a platform for constructing more complex 3D architectures *via* double B/N functionalization. While previous studies demonstrated B=N derivatization through the addition of a protic [H$^+$/OR$^-$] pair, we now show that two carbon-based fragments can be introduced in a nucleophile/electrophile sequence, enabled by an initial disruption of π-donation using organolithium reagents. This approach allowed the synthesis of BN-[4.4.4]-propellane as a model 3D B–N sp^3–sp^3 target, where the inherently unfavorable *trans*-diallylation was overcome through a metathesis-based isomerization and ring-closing strategy. While the 2D BN compound will likely continue to gain importance in organic opto-electronic design, we envisage that this and other synthetic strategies may help launch a new area of BN mapping of both known and unknown 3D cores.

Author contributions

G. S.-L.: methodology, investigation, writing–original draft, review and editing; J. S.: NMR methodology, writing of the section on lineshape analysis; P. N.: variable temperature NMR; A. B. C. and A. S.: project conception, methodology, supervision, management, writing–original manuscript, revisions and final version. A. S. was also responsible for DFT calculations.

Conflicts of interest

There are no conflicts to declare.

Data availability

CCDC 2470569 and 2470570 contain the supplementary crystallographic data for this paper.[26a,b]

The datasets supporting this article have been uploaded as part of the supplementary information (SI). Supplementary information: experimental procedures and compound characterization, NMR data (including VT NMR), as well as details on computational modelling by DFT. See DOI: **https://doi.org/10.1039/d5sc05132k**.

Acknowledgements

This work was supported through MICINN grant PID2020-113661GB-I00, MCIU grants PID2023-146324NB-I00 and PDC2023-145801-I00, and through AGAUR (2021 SGR 00520). We thank the Generalitat de Cataluña (AGAUR) for the Investigo contract to G. S.-L. (2023 INV-2 00014G1). We thank Dr János Rohonczy for his initial assistance in setting up the DNMR analysis.

Notes and references

1 (*a*) S. J. Blanksby and B. Ellison, *Acc. Chem. Res.*, 2003, **36**, 255–263; (*b*) R. H. Pritchard and C. W. Kern, *J. Am. Chem. Soc.*, 1969, **91**, 1631–1635; (*c*) I. Alkorta and J. Elguero, *Struct. Chem.*, 1998, **9**, 59–63.

2 (*a*) L. R. Thome, R. D. Suenram and F. J. Lovas, *J. Chem. Phys.*, 1983, **78**, 167–171; (*b*) M. Sugie, H. Takeo and C. Matsumara, *Chem. Phys. Lett.*, 1979, **64**, 573–575.

3 (*a*) C. R. McConnell and S.-Y. Liu, *Chem. Soc. Rev.*, 2019, **48**, 3436–3453; (*b*) A. J. Fritsch, *J. Chem. Heterocycl. Compd.*, 1977, **30**, 381–440; (*c*) H. Helten, *Chem. Eur. J.*, 2016, **22**, 12972–12982; (*d*) E. R. Abbey, L. N. Zakharov and S.-Y. Liu, *J. Am. Chem. Soc.*, 2008, **130**, 7250–7252.

4 (*a*) J. Y. Wang and J. Pei, *Chin. Chem. Lett.*, 2016, **27**, 1139–1146; (*b*) J. Huang and Y. Li, *Front. Chem.*, 2018, **6**, 341; (*c*) T. Sakamaki, T. Nakamuro, K. Yamashita, K. Hirata, R. Shang, E. Nakamura, R. Shang and E. Nakamura, *Chem. Mater.*, 2021, **33**, 5337–5344; (*d*) M. Tasior and D. T. Gryko, *J. Org. Chem.*, 2016, **81**, 6580–6586.

5 S. Ko, S. Shin, E. Ahn, J. Lyu, J. Lee and J. Han, EP 3940805A1, Samsung Display Co., Ltd, 2022.

6 (*a*) P. G. Campbell, A. J. V. Marwitz and S.-Y. Liu, *Angew. Chem., Int. Ed.*, 2012, **51**, 6074–6092; (*b*) M. J. D. Bosdet, W. E. Piers, T. S. Sorensen and M. Parvez, *Angew. Chem., Int. Ed.*, 2007, **119**, 5028–5031; (*c*) T. Kaehler, M. Bolte, H. W. Lerner and M. Wagner, *Angew. Chem., Int. Ed.*, 2019, **58**, 11379–11384; (*d*) P. F. Zhang, J. C. Zeng, F. D. Zhuang, K. X. Zhao, Z. H. Sun, Z. F. Yao, Y. Lu, X. Y. Wang, J. Y. Wang and J. Pei, *Angew. Chem., Int. Ed.*, 2021, **60**, 23313–23319.

7 (*a*) F. Lovering, J. Bikker and C. Humblet, Escape from Flatland: Increasing Saturation as an Approach to Improving Clinical Success, *J. Med. Chem.*, 2009, **52**, 6752–6756; (*b*) F. Lovering, Escape from Flatland 2: Complexity and Promiscuity, *Med. Chem. Commun.*, 2013, **4**, 515–519.

8 (*a*) A. D. Rohr, J. W. Kampf and A. J. Ashe, *Organometallics*, 2014, **33**, 1318–1321; (*b*) F. Sun, L. Lv, M. Huang, Z. Zhou and X. Fang, *Org. Lett.*, 2014, **16**, 5024–5027.

9 F. Rulli, G. Sanz-Liarte, P. Roca, N. Martínez, V. Medina, R. Puig de la Bellacasa, A. Shafir and A. B. Cuenca, *Chem. Sci.*, 2024, **15**, 5674–5680.

10 B. Halton, R. Boese, D. Bläser and Q. Lu, An Improved Synthesis, Molecular-Structure, and Properties of 1,4-Dihydro-Dicyclopropa[b,g]naphthalene, *Aust. J. Chem.*, 1991, **44**, 265–276.

11 As a surrogate for the π bond energy, the rotation barrier in $H_2B{=}NH_2$ is ∼30 kcal mol^{-1}, less than half of that (∼65 kcal mol^{-1}) found for ethylene:D. D. J. Grant and D. A. Dixon, σ- and π-Bond Strengths in Main Group 3–5 Compounds, *J. Phys. Chem. A*, 2006, **110**, 12955–12962.

12 A. M. Dilmaç, E. Spuling, A. de Meijere and S. Bräse, Propellanes—From a Chemical Curiosity to "Explosive" Materials and Natural Products, *Angew. Chem., Int. Ed.*, 2017, **56**, 5684–5718.

13 J. B. Geri, E. Y. Aguilera and N. K. Szymczak, Difluoromethane as a precursor to difluoromethyl borates, *Chem. Commun.*, 2019, **55**, 5119–5122.

14 A. Abengózar, M. A. Fernández-González, D. Sucunza, L. M. Frutos, A. Salgado, P. García-García and J. J. Vaquero, C–H Functionalization of BN-Aromatics Promoted by Addition of Organolithium Compounds to the Boron Atom, *Org. Lett.*, 2018, **20**, 4902–4906.

15 A. Nakazaki, A. Mori, S. Kobayashi and T. Nishikawa, Diastereoselective synthesis of 3,3-disubstituted oxindoles from atropisomeric N-aryl oxindole derivatives, *Tetrahedron Lett.*, 2012, **53**, 7131–7134.

16 J. Altman, E. Babad, J. Pucknat, N. Reshef and D. Ginsburg, *Tetrahedron*, 1968, **24**, 975–998.

17 O. Ermer, R. Gerdil and J. D. Dunitz, *Helv. Chim. Acta*, 1971, **54**, 2476–2487.

18 For prior examples of transannulative ring closing metathesis, see: (*a*) K. Takao, R. Nanamiya, Y. Fukushima, A. Namba, K. Yoshida and K. Tadano, *Org. Lett.*, 2013, **15**, 5582–5585; (*b*) J. P. A. Harrity, M. S. Visser, J. D. Gleason and A. H. Hoveyda, *J. Am. Chem. Soc.*, 1997, **119**, 1488–1489; (*c*) J. A. Henderson and A. J. Phillips, *Angew. Chem., Int. Ed.*, 2008, **47**, 8499–8501.

19 For the development of this 3rd generation Ru catalyst, see: (*a*) J. A. Love, J. P. Morgan, T. M. Trnka and R. H. Grubbs, *Angew. Chem., Int. Ed.*, 2002, **41**, 4035–4037; (*b*) D. J. Walsh, S. H. Lau, M. G. Hyatt and D. Guironnet, *J. Am. Chem. Soc.*, 2017, **139**, 13644–13647.

20 For metathesis-based *cis–trans* isomerization, we also cannot rule out a sequence operating *via* ethylenolysis of the ring olefin groups as shown below:

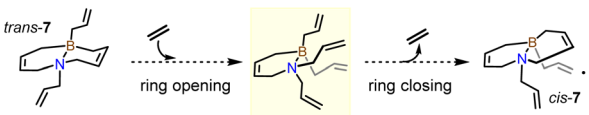

21 (*a*) S. H. Hong, M. W. Day and R. H. Grubbs, *J. Am. Chem. Soc.*, 2004, **126**, 7414–7415; (*b*) S. H. Hong, D. P. Sanders, C. W. Lee and R. H. Grubbs, *J. Am. Chem. Soc.*, 2005, **127**, 17160–17161.

22 (*a*) C. S. Higman, A. E. Lanterna, M. L. Marin, J. C. Scaiano and D. E. Fogg, Catalyst Decomposition During Olefin Metathesis Yields Isomerization-Active Ru Nanoparticles, *ChemCatChem*, 2016, **8**, 2446–2449, For a critical review of isomerization in metathesis,see; (*b*) B. J. van Lierop, J. A. M. Lummiss and D. E. Fogg, Ring-Closing Metathesis, in *Olefin Metathesis – Theory and Practice*, ed. K. Grela, Wiley, Hoboken, 2014, pp. 85–152.

23 (*a*) J. S. Murdzek and R. R. Schrock, *Organometallics*, 1987, **6**, 1373–1374; (*b*) R. R. Schrock, J. S. Murdzek, G. C. Bazan, J. Robbins, M. DiMare and M. O'Regan, *J. Am. Chem. Soc.*, 1990, **112**, 3875–3886; (*c*) G. C. Bazan, J. H. Oskam, H. N. Cho, L. Y. Park and R. R. Schrock, *J. Am. Chem. Soc.*, 1991, **113**, 6899–6907.

24 H. Gilboa, J. Altman and A. Loewenstein, *J. Am. Chem. Soc.*, 1969, **91**, 6062–6065.

25 H. Choo and J. Laane, The Barrier to Conformational Interconversion of Cyclohexene, *J. Am. Chem. Soc.*, 1994, **116**, 3889–3891.

26 (*a*) CCDC 2470569: Experimental Crystal Structure Determination, 2025, DOI: **10.5517/ccdc.csd.cc2nxts6**; (*b*) CCDC 2470570: Experimental Crystal Structure Determination, 2025, DOI: **10.5517/ccdc.csd.cc2nxtt7**.